

## Dynamics of low-energy heavy-ion fusion

A M STEFANINI

INFN-Laboratori Nazionali di Legnaro, I-35020 Legnaro, Padova, Italy

**Abstract.** Preliminary data on the fusion of  $^{36}\text{S} + ^{96}\text{Zr}$  are reported; the excitation function near the barrier is intermediate between those of  $^{40}\text{Ca} + ^{90,96}\text{Zr}$ . The peculiar role of the strong  $3^-$  octupole vibration of  $^{96}\text{Zr}$  is pointed out, in addition to the couplings to neutron transfer channels with positive  $Q$ -values. Recent data on  $^{40}\text{Ca} + ^{124}\text{Sn}$  are also shown; for that system the fusion barrier distribution is wide without separated peaks, similar to the case of  $^{40}\text{Ca} + ^{96}\text{Zr}$ . Simplified coupled-channel calculations have been performed, including surface vibrations and sequential neutron pick-up channels, with form factors that fit the single- and multi-nucleon transfer data for  $^{40}\text{Ca} + ^{124}\text{Sn}$ . A good agreement with the data is found.

**Keywords.** Heavy ions; sub-barrier fusion; barrier distributions.

**PACS No.** 25.70.Jj

### 1. Introduction

There has been considerable interest (and discussion) in recent years about the possibility of extracting fusion barrier distributions [1] from the fusion excitation functions in the energy range encompassing the Coulomb barrier. This procedure has actually yielded detailed information on the fusion dynamics in several heavy-ion systems [2,3], more detailed than what is possible to get from a simple analysis of the excitation functions and from their comparison with the theoretical models.

Here I present some recent experimental results in this field, which our group has obtained at the Laboratori Nazionali di Legnaro of INFN. The measurements of fusion-evaporation cross sections were performed using the XTU tandem accelerator.  $^{40}\text{Ca}$ ,  $^{36}\text{S}$  beams with intensities  $\sim 3\text{--}10$  pA; isotopically enriched targets were used, with thickness  $\sim 50\text{--}90$   $\mu\text{g}/\text{cm}^2$ , evaporated onto  $15$   $\mu\text{g}/\text{cm}^2$  carbon layers.

The evaporation residues (ER) were detected at  $0^\circ$  and at small angles by an energy time-of-flight telescope following an electrostatic beam deflector. Beam rejection factors  $\sim 10^7\text{--}10^8$  were achieved. Absolute cross section normalization was ensured by four monitor detectors mounted in a ring perpendicular to the beam direction, each one at a scattering angle  $\theta_{\text{lab}} = 22^\circ$ , and by measuring the transmission of the beam deflector for ER (usually around 60–70%). Particular attention was devoted to the quality of the beam and to the statistical accuracy of the measurements, which was  $\sim 1\%$  around and over the barrier. Excitation functions were measured at  $0^\circ$  only downwards in energy with 0.5 MeV steps (1.0 MeV for the highest energy points). Angular distributions of ER were measured at

selected energies around and above the barriers in the range  $0^\circ$ – $7^\circ$  with  $1^\circ$  steps. See ref. [4] for more details.

## 2. Fusion with $^{90,96}\text{Zr}$ targets

The results of a detailed study of the two systems  $^{40}\text{Ca} + ^{90,96}\text{Zr}$  were published recently [5]. Since the projectile  $^{40}\text{Ca}$  is a magic nucleus, its influence on fusion was expected to be small, whereas both targets  $^{90,96}\text{Zr}$  have a  $Z = 40$  subshell closure. A main difference between the two reactions is in the neutron transfer  $Q$ -values which are very positive, in the case of  $^{96}\text{Zr}$  only, up to the pickup of 8 neutrons. However, a further aspect was not considered fully in that work; while the low-lying quadrupole vibrations of  $^{90}\text{Zr}$  and  $^{96}\text{Zr}$  are found at similar excitation energies and are only moderately collective,  $^{96}\text{Zr}$  has an octupole vibration significantly stronger and lower-lying than the corresponding state in  $^{90}\text{Zr}$ .

Figure 1a shows the two measured excitation functions on a reduced energy scale. A very large relative enhancement is observed for  $^{40}\text{Ca} + ^{96}\text{Zr}$  at low energies. The corresponding barrier distribution plotted in figure 1c has a flat and rather structureless shape extending to very low energies. It is qualitatively different from the distribution for  $^{90}\text{Zr}$  (see figure 1b), which shows well defined peaks. The barrier structure and fusion excitation function of  $^{40}\text{Ca} + ^{90}\text{Zr}$  were explained in terms of coupling to the low-lying inelastic excitations of  $^{90}\text{Zr}$  (solid lines in figure 1a,b), but these couplings could not explain the fusion of  $^{40}\text{Ca} + ^{96}\text{Zr}$ . Calculations [5] indicate that sequential neutron transfer is required to explain the observed distribution.

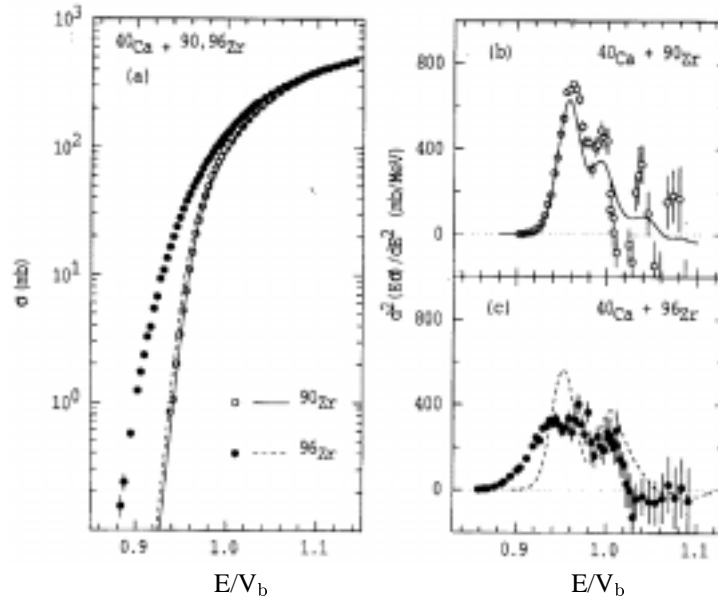


**Figure 1.** The fusion excitation functions and barrier distributions for  $^{40}\text{Ca} + ^{90,96}\text{Zr}$  [5]. The CC calculations for  $^{90}\text{Zr}$  (solid) and  $^{96}\text{Zr}$  (dashed) including the inelastic excitations of the Zr nuclei are shown. Taken from [3].

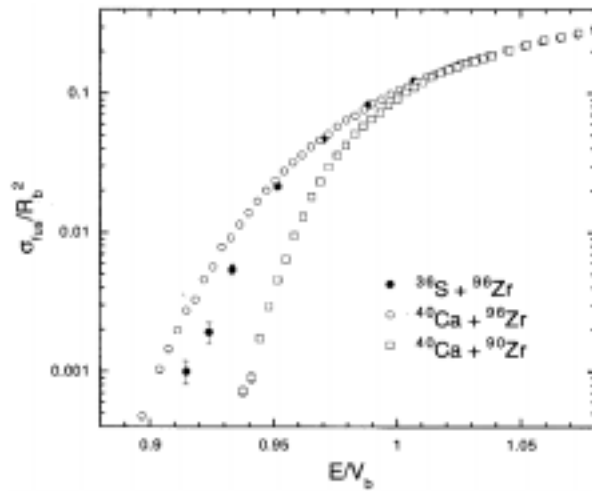


**Figure 2.** The fusion excitation functions for  $^{36}\text{S} + ^{96}\text{Zr}$  and for  $^{40}\text{Ca} + ^{90,96}\text{Zr}$  in a reduced scale.

In this context, it seemed important to us to try to assess experimentally the effect of the strong octupole vibration of  $^{96}\text{Zr}$  on fusion. That is surely one reason for the relative enhancement of  $^{40}\text{Ca} + ^{96}\text{Zr}$  compared to  $^{40}\text{Ca} + ^{90}\text{Zr}$ , since, qualitatively speaking, one expects that the octupole shape strongly favours sub-barrier fusion. It is worthwhile pointing out, more is general, that there is little clear-cut available data in the literature about the influence of octupole vibrations on fusion, probably because either they are too high in energy, or their role is mixed up and surmounted by lower-lying quadrupole vibrations.

The case of  $^{96}\text{Zr}$  is a promising one, since the  $3^-$  state is relatively low and very strong ( $\beta = 0.34$ ). The system  $^{36}\text{S} + ^{96}\text{Zr}$  was considered, where, in comparison with  $^{40}\text{Ca} + ^{96}\text{Zr}$ , we have a similar rigid projectile structure (the rather strong  $3^-$  state of  $^{40}\text{Ca}$  is high in energy, and its effect on fusion is anyway taken into account), but no transfer channels with positive or even slightly negative  $Q$ -values are available. Hence, we expect for  $^{36}\text{S} + ^{96}\text{Zr}$  less sub-barrier fusion and, possibly, a barrier distribution with sharp and separated peaks, at variance with the case of  $^{40}\text{Ca} + ^{96}\text{Zr}$ ; the effect of the octupole coupling, if any, may be better isolated.

A preliminary experiment has been performed for  $^{36}\text{S} + ^{96}\text{Zr}$ , and the measured cross sections are shown in figure 2, together with the previous results for the two Ca + Zr systems. The  $^{36}\text{S} + ^{96}\text{Zr}$  cross sections are found to be intermediate between those of the other two systems, nearer to the  $^{40}\text{Ca} + ^{96}\text{Zr}$  excitation function. A more detailed study of  $^{36}\text{S} + ^{96}\text{Zr}$  will be performed at LNL soon, with small energy steps and high statistical accuracy, to enable us to extract the barrier distribution from the second derivative of the excitation function.

### 3. The case of $^{40}\text{Ca} + ^{124,(116)}\text{Sn}$

Large multinucleon transfer cross sections were measured for  $^{40}\text{Ca} + ^{124}\text{Sn}$  [6] a couple of years ago, as well as, more recently, for  $^{40}\text{Ca} + ^{96}\text{Zr}$  [7]. A proton-rich projectile ( $^{40}\text{Ca}$ )

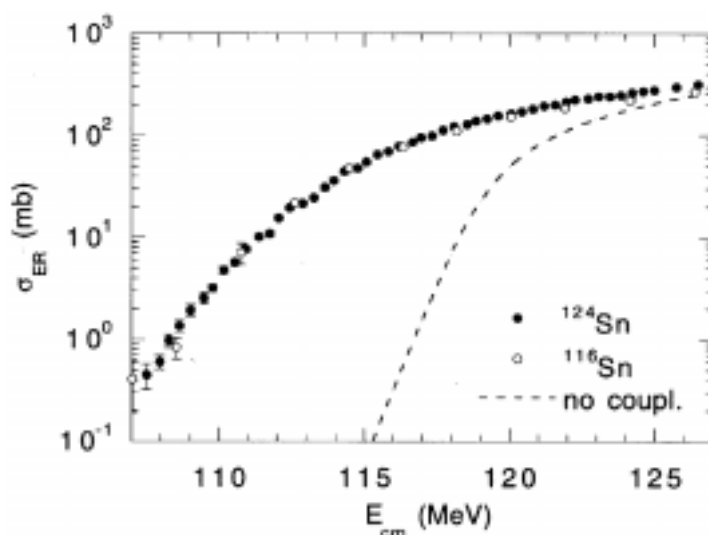


**Figure 3.** The fusion excitation functions for  $^{40}\text{Ca} + ^{124,(116)}\text{Sn}$ .

collides with neutron-rich targets, hence the  $Q$ -values for neutron pick-up channels are very positive in both cases, ranging from  $\approx +5$  MeV to  $\approx +12$  MeV for the transfer of up to 8 neutrons. It is interesting to point out that the angle- and  $Q$ -integrated cross sections for each individual transfer channel are very similar in the two systems.

The measurement of fusion-evaporation cross sections of  $^{40}\text{Ca} + ^{124}\text{Sn}$  was recently performed at LNL, in the relevant energy range near the Coulomb barrier. The resulting evaporation residue (ER) cross sections are plotted in figure 3; since the fusion-fission cross sections are estimated to be very small (only a few mb at the highest energies), the data can be considered total fusion cross sections with little uncertainty. At selected energies, ER yields were also measured for the  $^{40}\text{Ca} + ^{116}\text{Sn}$  systems. These are reported in figure 3 too, with a small shift of the energy to compensate for the Coulomb barrier difference between the two cases.

The two excitation functions overlap almost perfectly. We know that the nuclear structures of  $^{124}\text{Sn}$  and  $^{116}\text{Sn}$  are very similar; the  $Q$ -values for neutron pick-up in  $^{40}\text{Ca} + ^{116}\text{Sn}$  are positive ( $\approx 2$ – $3$  MeV), although not so large as in the reaction with  $^{124}\text{Sn}$ . One may argue that either such transfer processes do not influence at all the fusion dynamics, or that their effect (if significant) is very similar in the two cases. An analogous situation was found in the study of  $^{40}\text{Ar} + ^{112,116,122}\text{Sn}$  by Reisdorf *et al* [8]. It is possible, for  $^{40}\text{Ca} + ^{124}\text{Sn}$  only, to extract the barrier distribution from the data. The case of  $^{40}\text{Ca} + ^{116}\text{Sn}$  needs a more detailed experimental study, i.e. many more points around and below the barrier.

Since one has very similar  $Q$ -values for few- and multi-nucleon transfer channels in  $^{40}\text{Ca} + ^{96}\text{Zr}$ ,  $^{124}\text{Sn}$ , it is interesting to compare their behaviour as far as fusion is concerned. Figure 4 shows the excitation functions in a reduced energy scale (top): the sub-barrier cross sections of  $^{40}\text{Ca} + ^{96}\text{Zr}$  are significantly larger. The two barrier distributions are reported in the lower part of figure 4. As in the case of  $^{40}\text{Ca} + ^{96}\text{Zr}$ , no defined peak is

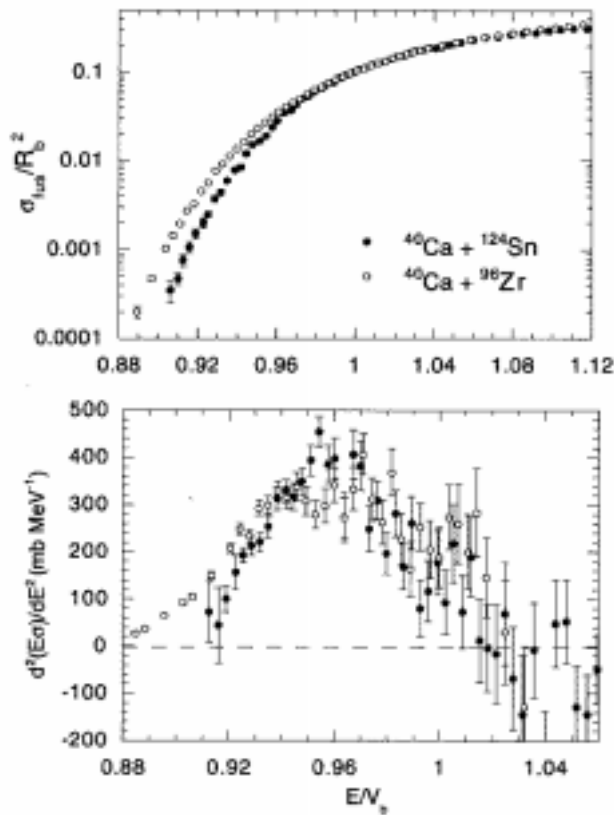


**Figure 4.** The reduced fusion excitation functions of  $^{40}\text{Ca} + ^{124}\text{Sn}$ ,  $^{96}\text{Zr}$  (top), and the corresponding barrier distributions (down).

seen in the distribution for  $^{40}\text{Ca} + ^{124}\text{Sn}$  and an overall bump-like shape is observed for both systems.

The distribution for  $^{40}\text{Ca} + ^{96}\text{Zr}$  extends slightly farther down in energy. The underlying reason(s) are not clear at this level, and a consideration of the  $Q$ -value and angle-integrated transfer cross sections for the two systems does not help in this respect. Actually the mass and  $Z$  distributions of Ca-like ejectiles are very similar in the two systems, as stated above; the yields of corresponding nuclides rarely differ by more than a factor two. Hence, the mechanism leading to larger sub-barrier fusion cross sections in  $^{40}\text{Ca} + ^{96}\text{Zr}$  might be looked for elsewhere. A possibility, supported by calculations, is the very strong octupole vibration of  $^{96}\text{Zr}$  at  $\sim 1.8$  MeV; the corresponding excitation in  $^{124}\text{Sn}$  is much less collective and is found at  $\sim 2.6$  MeV.

#### 4. Analysis with simplified coupled-channel calculations

Simplified coupled-channels (CC) calculations have been performed for  $^{40}\text{Ca} + ^{124}\text{Sn}$  with the code CCMPH [9], which allows for multi-phonon and multinucleon transfer modes to

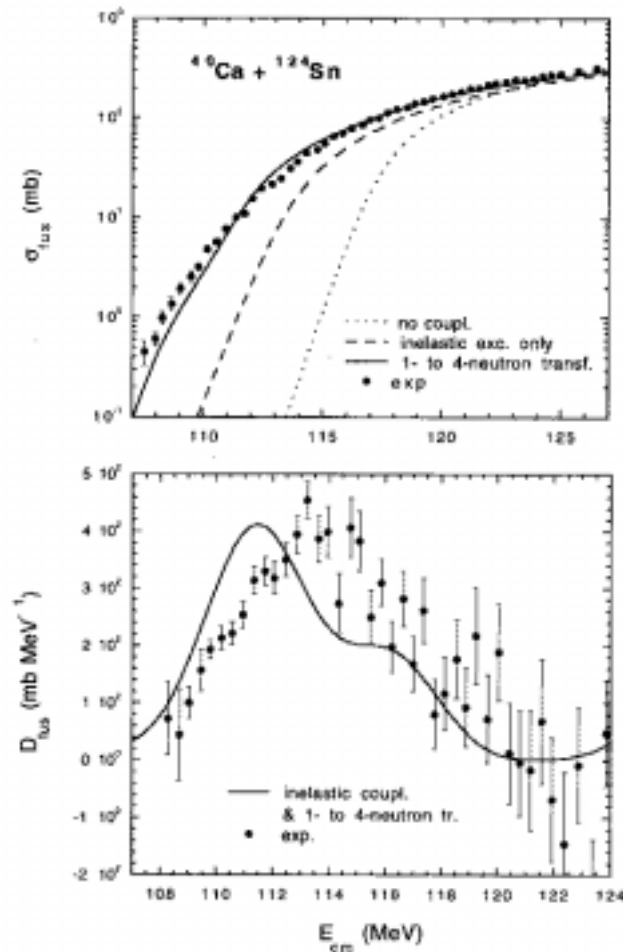


**Figure 5.** The fusion excitation function of  $^{40}\text{Ca} + ^{124}\text{Sn}$ , (top), and the corresponding barrier distribution (down), compared with the results of coupled-channel calculations (see text).

be coupled in. As far as inelastic excitations are concerned, the lowest  $2^+$  and  $3^-$  states of  $^{124}\text{Sn}$  have been included, together with the strong octupole vibration of  $^{40}\text{Ca}$ , although it lies rather high in energy. The Akyüz–Winther potential has been used, with a slightly larger diffusivity  $a = 0.76$  fm. The mutual excitations of the Ca and Sn states have been considered too.

Sequential transfer of up to four neutrons has been included in the coupling scheme. The form factors for single-neutron pick-up are the same as used in ref. [6], which lead to a good agreement with the experimental transfer cross section and  $Q$ -value distribution. They were derived following Quesada *et al* [10] and include a set of transitions from six shell model states in  $^{123}\text{Sn}$  ( $1h_{11/2}$ ,  $2d_{3/2}$ ,  $3s_{1/2}$ ,  $2d_{5/2}$ ,  $1g_{7/2}$ ,  $1g_{9/2}$ ) to four states in

$^{41}\text{Ca}$  ( $1f_{5/2}, 2p_{1/2}, 2p_{3/2}, 1f_{7/2}$ ). Here the single form factors have been combined into one effective form factor, as a quadratic sum of the individual ones. This effective one-neutron form factor  $F_{1n}$  is close to 3 MeV at the barrier radius. For the  $2n, 3n$  and  $4n$  pick-up channels, whose  $Q_{gs}$  are large and positive, the prescription of Broglia *et al* [11] has been used, which leads to  $F_{2n} = \sqrt{2} \times 3/2 F_{1n}$ ,  $F_{3n} = \sqrt{3} \times 13/6 F_{1n}$  and  $F_{4n} = 73/12 F_{1n}$ . In the CCMPH calculations, zero  $Q$ -values (close to the optimum  $Q$ -values) were attributed to all of these channels.

The results of the CCMPH calculations are shown in figure 5. The fusion excitation function is in good agreement with the data, and it shows that large enhancements are produced both by inelastic excitations and by neutron transfer channels; the role of proton stripping channels should be investigated as well. However, the calculated barrier distribution looks like shifted in energy with respect to the 'experimental' one, although having an overall correct shape.

We see, anyway, that the complete and detailed sets of data obtained for  $^{40}\text{Ca} + ^{124}\text{Sn}$  (and for other few cases as well) are suitable for a unified treatment of all the reaction channels. It seems particularly interesting to me the use of form factors that fit the experimental transfer data, for the coupled-channel calculation of fusion at low energies.

The simplified CC approach we have followed in the analysis of the present  $^{40}\text{Ca} + ^{124}\text{Sn}$  system suffers from various approximations, and hence no defined conclusion should be drawn out of it. But I feel it is a step in the right direction, in order to better understand the dynamics of low-energy fusion.

## Acknowledgements

The author is pleased to acknowledge the collaboration with his experimental colleagues D Ackermann, S Beghini, L Corradi, C J Lin, G Montagnoli, F Scarlassara, G F Segato and L F Zheng. He is also very grateful to G Pollarolo and N Rowley for many fruitful discussions.

## References

- [1] N Rowley, G R Satchler and P H Stelson, *Phys. Lett.* **B254**, 25 (1991)
- [2] Proc. Int. Workshop on Heavy-Ion Collisions at Near-Barrier Energies, South Durras, NSW, Australia, March 17–21, 1997, *J. Phys. G: Nucl. Part. Phys.* **23** (1997)
- [3] M Dasgupta, D J Hinde, N Rowley and A M Stefanini, *Ann. Rev. Nucl. Part. Sci.* (1998) in press
- [4] A M Stefanini, D Ackermann, L Corradi, D R Napoli, C Petrache, P Spolaore, P Bednarczyk, H Q Zhang, S Beghini, G Montagnoli, L Müller, F Scarlassara, G F Segato, F Soramel and N Rowley, *Phys. Rev. Lett.* **74**, 864 (1995)
- [5] H Timmers, D Ackermann, S Beghini, L Corradi, H J He, G Montagnoli, F Scarlassara, A M Stefanini and N Rowley, *Nucl. Phys.* **A633**, 421 (1998)
- [6] L Corradi, J H He, D Ackermann, A M Stefanini, A Pisent, S Beghini, G Montagnoli, F Scarlassara, G F Segato, G Pollarolo, C H Dasso and A Winther, *Phys. Rev.* **C54**, 201 (1996)
- [7] G Montagnoli, S Beghini, F Scarlassara, G F Segato, L Corradi, C J Lin and A M Stefanini, *J. Phys. G: Nucl. Part. Phys.* **23**, 1431 (1997)
- [8] W Reisdorf, F P Hessberger, K D Hildenbrand, S Hofmann, G Münzenberg, K-H Schmidt, J H R Schneider, K Sümmerer, G Wirth, J V Kratz and K Schlitt, *Nucl. Phys.* **A438**, 212 (1985)

- [9] M Dasgupta *et al*, *Nucl. Phys.* **A539**, 351 (1992); ANU Int. Rep. ANU P/1333 (1997)
- [10] J M Quesada, G Pollarolo, R A Broglia and A Winther, *Nucl. Phys.* **A442**, 381 (1985)
- [11] R A Broglia, C H Dasso, G Pollarolo and A Winther, *Phys. Rep.* **48**, 378 (1978)